Available online at www.sciencedirect.com
SCIENCE DIRECT®
Thermochimica Acta 423 (2004) 99–106
thermochimica acta
www.elsevier.com/locate/tca

Effects of oxidative treatments with air and CO_2 on vapour grown carbon nanofibres (VGCNFs) produced at industrial scale

A. Arenillas [a], S. Cuervo [a], A. Domínguez [a], J.A. Menéndez [a,*], F. Rubiera [a], J.B. Parra [a], C. Merino [b], J.J. Pis [a]

[a] *Instituto Nacional del Carbón (INCAR), CSIC, Apartado 73, 33080 Oviedo, Spain*
[b] *Grupo Antolín Ingeniería, S.A., Ctra. Madrid-Irún, km. 2448, 09007 Burgos, Spain*

Received 13 February 2004; received in revised form 26 April 2004; accepted 5 May 2004
Available online 28 July 2004

Abstract

Vapour grown carbon nanofibres (VGCNFs) produced at industrial scale were subjected to different treatments in N_2, air and CO_2 atmospheres. The effect of these treatments on the homogeneity of the industrial product was investigated by means of TG analysis. Temperature programmed oxidation (TPO) experiments were performed to obtain DTG profiles. The DTG curves were deconvoluted into a mixture of Gaussian–Lorentzian curves, so that the contribution of each peak could be evaluated and assigned to phases of different reactivity. It was found that treatments in air are more selective in removing the most reactive phase (which has a higher content of amorphous carbon) at low burn-off, while at an elevated burn-off degree CO_2 treatments result in a greater enrichment of the product in the less reactive phase (which has a higher content of fibre). This behaviour is attributed to the presence of a certain amount of iron in the industrially produced materials and its catalytic effect on the oxidative reactions. The effect of the treatments on the porous texture, surface chemistry and graphite-like character of the samples was also investigated.

Keywords: Vapour grown carbon nanofibres (VGCNFs); Reactivity; DTG

1. Introduction

Vapour grown carbon nanofibres (VGCNFs) are a relatively new type of carbon fibre, which is produced from the pyrolysis of hydrocarbon gases, such as benzene, methane, acetylene, etc., in the presence of hydrogen at temperatures around 950–1200 °C [1–6]. The fibre growth is initiated by ultrafine transition metal catalyst particles, usually Fe, Co, Ni, deposited on a substrate (seeded catalyst method) or directly injected into the gas (floating catalyst method) [1].

These fibres have been characterised in terms of the highly preferred orientation of their graphitic basal planes parallel to the fibre axis with an annular ring texture in the cross section. This structure gives rise to excellent mechanical properties and very high electrical and thermal conductivity [2,3]. These properties lie somewhere between those of commercial ex-PAN or pitch carbon fibres and carbon nanotubes. Due to these properties VGCNFs have been used to produce polymer composites with an improved tensile strength and tensile modulus and a better electrical and thermal conductivity. Other applications of this material include its use in tires partially to replace carbon blacks thereby adding a greater wear resistance, or in lithium ion batteries because carbon nanofibres are easily intercalated with Li ions [7].

Various carbon sources and catalysts can be used for VGCNF production. Especially suitable due to their catalytic activity are Fe, Co and Ni [8–10]. It is unlikely that carbon nanofibres grow directly from the initial carbon source. In fact, they are thought to be obtained from secondary products generated from the decomposition of the initial carbon source. Due to the complexity of the gaseous reactions that take place, VGCNFs can be massively produced at the expense of product quality [11]. The main problem with the industrial-scale production of this kind of fibres is the heterogeneity of the product, i.e., fibres of a wide range of size mixed with pyrolytic, amorphous and probably other carbon forms.

* Corresponding author. Tel.: +34-985-118972; fax: +34-985-297662.
E-mail address: angelmd@incar.csic.es (J.A. Menéndez).

0040-6031/$ – see front matter © 2004 Elsevier B.V. All rights reserved.
doi:10.1016/j.tca.2004.05.002

For most commercial applications it is necessary to increase the percentage of VGCNFs in the industrially fabricated product and sometimes it is important to obtain fibres with a narrow distribution of sizes, then VGCNFs have to be upgraded, for example, by applying different treatments based on the preferential oxidation of unwanted components with air or other oxidising agents. These treatments may also serve to functionalise the carbon fibres, increasing the interaction between the fibre and the matrix in the subsequent fabrication of composites.

There is no established technique to determine the relative amount of VGCNFs in an industrial product that contains different impurities or to quantify the real effect of the treatments performed to increase the percentage of the VGCNFs in the fabricated material. However, thermogravimetric analysis has been used to assess the amount of nanotubes produced at large scale [12] and to analyse the purity of carbon nanotubes attained after different purification processes [13–15].

The aim of this work was to evaluate the effect of treating VGCNFs obtained at industrial-scale by heating them in oxidising atmospheres (air and CO_2) in order to preferentially remove unwanted components and to increase the percentage of the desired fibres in the final product. In addition, the application of thermogravimetric techniques in order to quantify the relative amount of fibres in the industrially produced raw material and in the product subsequently treated by oxidative treatments was also evaluated.

2. Experimental

2.1. Materials

The material studied in this work was obtained in an industrial-scale furnace with an inner diameter of 400 mm and a reaction length of 4500 mm. Its length was divided into nine heating zones of 500 mm. The operating temperature was 1100 °C, and the electrical power for heating was 109 kW [16]. The production of VGCNFs was based on the floating catalyst method reported in the literature and patents [8,9,17]. The process was carried out by introducing the carbon source (i.e., methane), the iron based catalyst and hydrogen from the top of the furnace. The product was separated from the exhaust gases at the bottom of the furnace by a filtering system and a pneumatic piston that allowed the carbon nanofibres to be collected without compromising the gas tightness of the furnace.

Due to the large size and the innovative concepts introduced in the design of the furnace by Grupo Antolin Ingeniería, S.A. [16], it was difficult to optimise the manufacturing parameters to obtain VGCNFs of a high purity. In the first manufacturing trials the product obtained (FGA) was characterised by fibres with diameters in the range 50–500 nm and lengths of 50–100 μm. However, the product also presented significant amounts of other forms of carbon (i.e., amorphous carbon, pyrolytic carbon, etc.) as can be seen in the SEM micrograph of the raw material shown in Fig. 1a. Similarly, the proximate analysis presented in Table 1 shows that the initial FGA product exhibits 12.4% of volatile matter (VM).

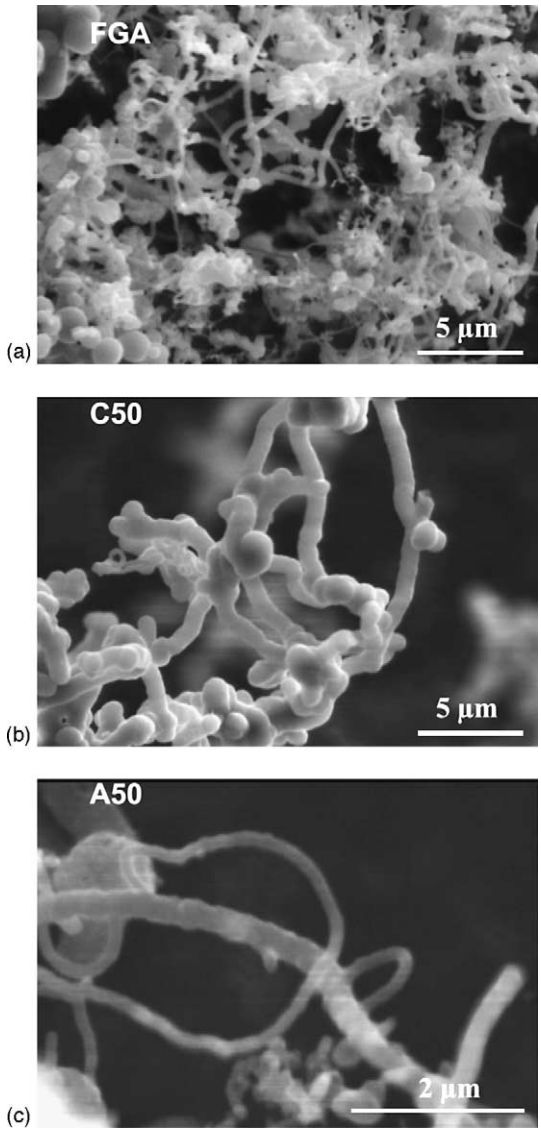

Fig. 1. SEM microphotographs of selected samples.

2.2. Thermal treatments

The initial product, FGA, was subjected to partial oxidation by thermal treatment under air and CO_2 atmospheres in order to purify the VGCNFs of other forms of carbon. The procedure involved the use of approximately 700 mg of FGA fibres which were introduced into a 2.5 cm internal diameter, 65 cm length quartz reactor, externally heated by an electric furnace. The samples were heated from room temperature up to the treatment temperatures (600 °C in the case of air and 900 °C in the case of CO_2), under a nitrogen

Table 1
Chemical characterisation of the parent and treated fibres

	Proximate analysis (%)			Ultimate analysis (%daf)					pH_{PZC}
	Moisture	VM (db)	Ash (db)	C	H	N	S	O	
FGA	0.2	12.4	2.3	98.6	0.6	0.6	0.0	0.2	8.0
N600	1.2	4.1	3.0	99.0	0.4	0.0	0.0	0.5	7.5
N900	0.7	5.5	3.2	99.1	0.3	0.0	0.0	0.5	7.6
C50	0.5	2.4	5.9	99.2	0.2	0.0	0.0	0.6	7.7
C80	0.1	n.d.	9.3	99.1	0.2	0.0	0.0	0.7	7.7
A50	3.9	7.7	6.2	99.3	0.4	0.0	0.0	0.2	7.8
A80	3.9	n.d.	16.8	99.1	0.2	0.0	0.0	0.6	7.3

n.d.: not determined; db: dry basis; daf: dry and ash-free basis.

flow rate of 50 mL min^{-1}. These temperatures were previously chosen by subjecting the raw fibre to temperature programmed oxidation (TPO) tests in air and in CO_2 in a thermogravimetric system, the procedure for which is described below.

The oxidation treatments were carried out with a gas flow rate of 30 mL min^{-1} (air) or 10 mL min^{-1} (CO_2). In both cases the treatment times were varied in order to obtain samples with 50 and 80% burn-off degrees (A50, A80 for the air-treated samples and C50, C80 for the CO_2-treated samples). During the heating and cooling-down periods a nitrogen flow rate of 50 mL min^{-1} was allowed to pass through the reactor. Samples treated under nitrogen at 600 and 900 °C (denoted as N600 and N900) were also obtained for comparative purposes. It should be noted that these high burn-off degrees are probably unrealistic from an industrial point of view. They were chosen, however, in order to magnify the different effects produced on the fibres so that the processes could be more easily examined.

2.3. Thermogravimetric analysis

Thermogravimetric analysis is a useful technique for studying the thermal behaviour of carbon materials; it has also been used to quantitatively evaluate the relative purity of raw and processed carbon nanotubes [13,14]. However, the well-controlled conditions encountered in TGA systems need to be optimised for each study, due to their important effect on the results obtained. The heating rate, the flow rate of the gases and the amount of sample must be well-established in order to prevent any possible restriction to mass transfer through the samples, and to obtain well-resolved peaks on the DTG curves. In accordance with previous studies [18,19] a heating rate of 15 °C min^{-1}, and an air flow rate of 50 mL min^{-1} were used for the TPO tests.

The influence of the amount of sample used can be observed in Fig. 2a, where TPO tests in air for two different initial masses of raw fibres (FGA) are displayed. A high sample mass leads to diffusional constraints with wide unresolved peaks, whereas a small sample mass (i.e., 3 mg) produces two different peaks, although there is some overlap between the two oxidation stages.

The DTG oxidation profile of the raw fibre in CO_2 is presented in Fig. 2b. It can be observed that the reaction rate is slower and the profile shifts to a higher temperature when carbon dioxide is used. In contrast, the oxidation profile in air shows that the oxidation proceeds in two well-defined stages. This suggests that the least reactive carbon could be preferentially removed by setting the oxidation temperature at a value between the low and high temperature stages. In this work the temperature chosen for the oxidation tests in the quartz reactor was that needed to reach half the value of the maximum rate of mass loss in the DTG profiles, i.e., 600 °C in air or 900 °C in CO_2.

2.4. Porous texture, morphological and chemical characterisation

The textural characteristics of the samples were determined by nitrogen physisorption at 77 K, performed in a Micromeritics ASAP 2000 apparatus. The apparent surface area (S_{BET}) and the total specific pore volume (v_p) were evaluated using the modified BET equation [20] and the Gurvitsch rule [21], respectively. The total specific pore volume was calculated as the liquid volume adsorbed at a predetermined p/p° of 0.95. The results are shown in Table 2.

XRD patterns were achieved with a Siemens D5000 diffractometer using Cu Kα radiation (30 mA, 40 kV) as an X-ray source. The scans were carried out over an angular range of 10–90° 2θ in continuous scan mode with a step size of 0.02° (2θ). Scattered X-ray intensities were collected for

Table 2
Porous texture and structural parameters of the parent and treated fibres

Sample	Porous texture parameters		Structural parameters	
	S_{BET} ($m^2\ g^{-1}$)	v_p ($cm^3\ g^{-1}$)	d_{002} (Å)	Lc (Å)
FGA	5	0.005	3.53	26
N600	6	0.005	3.51	28
N900	5	0.005	3.51	28
C50	7	0.013	3.50	28
C80	8	0.017	3.53	28
A50	16	0.017	3.51	27
A80	12	0.014	3.52	27

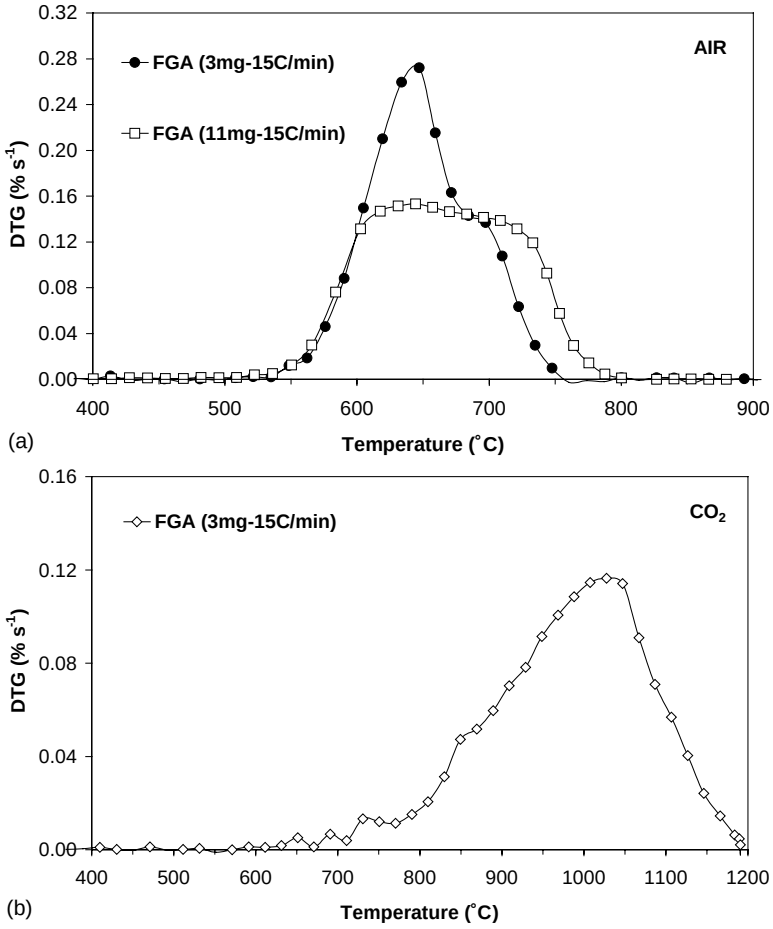

Fig. 2. DTG profiles under different conditions in (a) air and (b) CO_2.

2 s at each step. X-ray structural parameters (d_{002}, Lc) were obtained through the analysis of the (0 0 2) line profile using the Bragg equation [22] to evaluate the interlayer spacing (d), and the Debye–Scherrer equation [23] to evaluate the crystallite size of the stacks (Lc). Fig. 3 shows XRD plots of the samples and Table 2 shows the values of the structural parameters obtained. Ultimate analysis of all the samples was carried out in a LECO CHNS-932 analyser coupled to a LECO VTF-900 pyrolysis furnace, which enabled the oxygen content to be determined directly. The point of zero charge (pH_{PZC}) of each sample was assessed by using a modified version of a simple method proposed by Noh and Schwarz [24], referred to as reverse mass titration [25].

3. Results and discussion

The DTG air oxidation profile of the raw fibre, FGA, presented in Fig. 4 indicates that there are, at least, two easily distinguishable steps. The figure also displays the curves obtained by deconvoluting the DTG curve into a mixture of Gaussian–Lorentzian curves. The two curves correspond to the two main constituents of the FGA fibre. This does not imply that there are only two carbon forms in the product, but merely the presence of two products, which may include more than one component, with clearly different oxidation reactivities.

The two peaks on the DTG curve are centred at around 640 and 700 °C. According to the SEM micrographs of Fig. 1a, disordered carbon (i.e., amorphous carbon) is present in the industrial product and it is well-known that this type of carbon is more reactive than the carbon fibre. The first peak, which corresponds to the most reactive fraction of the carbon is assumed to have a higher amorphous carbon content. The second peak, on the other hand, corresponds to the less reactive components. These can be assigned mainly to the carbon fibre and spherules of pyrolytic carbon, which were also detected by SEM (Fig. 1a). Moreover, the catalytic effect of the iron in these samples, which also influences the reactivity (see below), must also be taken into account.

Table 3 shows the contribution of each deconvoluted peak, calculated on an area basis, to the reactivity profile of the raw material. Thus, the low-temperature peak (i.e., formed by the most reactive components) provides a contribution of 80% versus 20% from the high temperature peak, which corresponds to the less reactive carbon form.

The thermal treatment of the raw material in an inert atmosphere do not seem to modify to any great extent

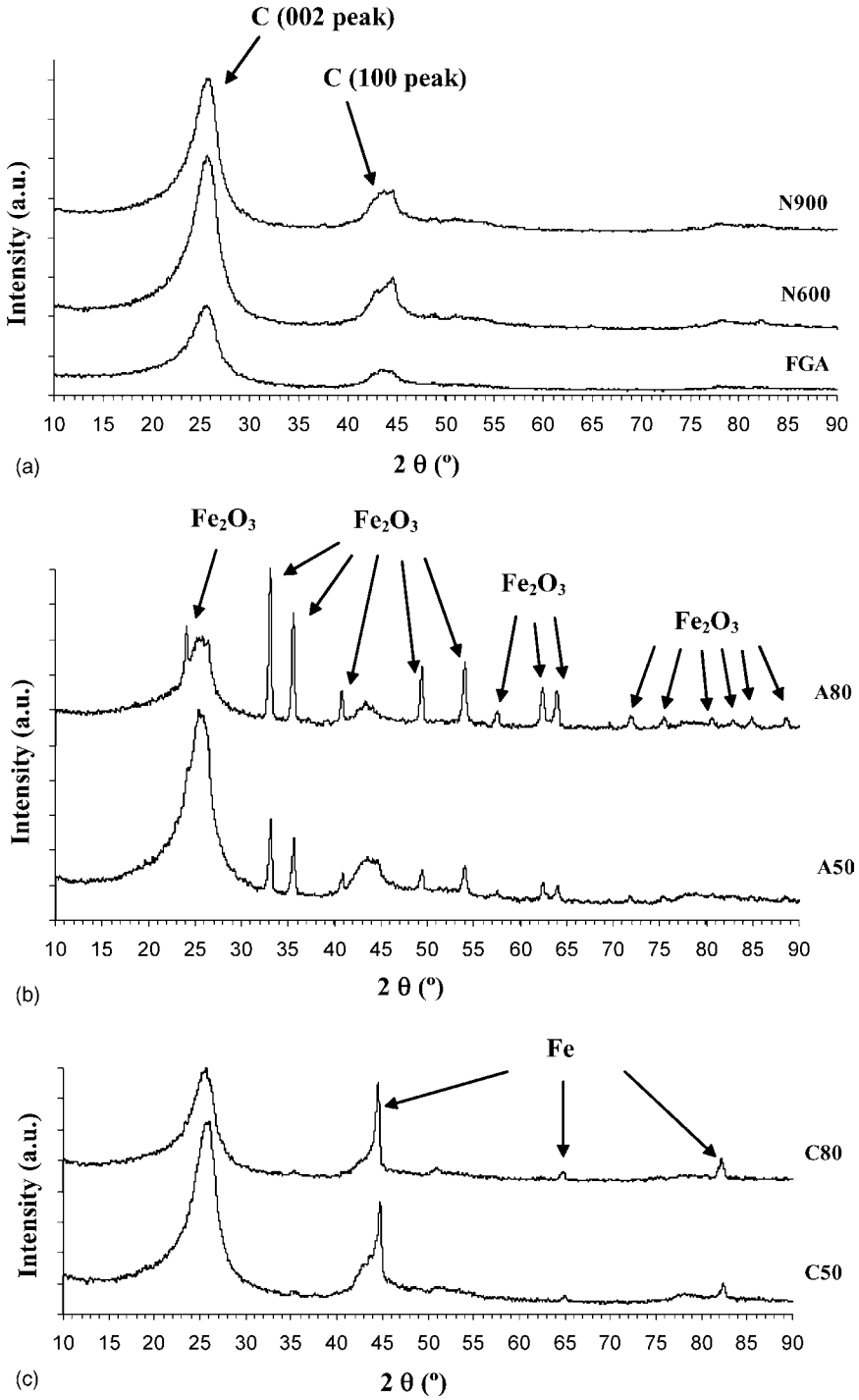

Fig. 3. X-ray diffraction patterns of (a) untreated and nitrogen-treated samples, (b) air-treated samples and (c) CO_2-treated samples.

the heterogeneity of the sample. A bimodal peak was also observed for samples N600 and N900, with a similar contribution of the deconvoluted peaks to that of the raw material (Table 3). The main effect of the thermal treatment on the reactivity behaviour of the initial product was to shift the end of the rate of mass loss to higher temperatures, probably due to thermal annealing of some of the carbon structures. Therefore, heat treatment in an inert atmosphere does not increase the relative concentration of the fibres with respect to the parent sample.

The reactivity profiles of the samples treated in CO_2 at two different degrees of burn-off (50 and 80%) are presented in Fig. 5. It can be seen that treatment in this reactive atmosphere also shifts the end of the rate of mass loss to slightly higher temperatures with respect to the profile of the raw material (Fig. 4). This can be explained if one considers

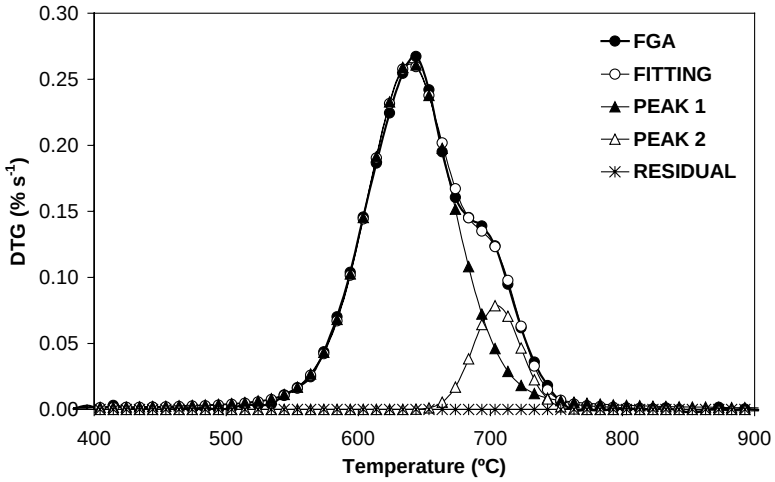

Fig. 4. Example of deconvolution of a DTG profile (sample FGA).

Table 3
Relative contribution of the peaks obtained from the deconvolution of the reactivity profiles of the fibres studied

Sample	Peak 1	Peak 2
FGA	80	20
N600	81	19
N900	80	20
C50	73	27
C80	8	92
A50	55	45
A80	20	80

that, besides the elimination of the most reactive phase by reaction with CO_2, the sample was maintained at high temperature (i.e., 900 °C), which can cause certain degree of thermal annealing.

A clear difference between the oxidation profiles of the samples treated at 50 and 80% of burn-off can be observed. Thus, while sample C50 presents a bimodal peak with an important contribution from the peak at low temperature (73% according to Table 3), sample C80 presents a single peak at 700 °C with a very small contribution (8%; see Table 3) from the low-temperature peak. This indicates that the homogeneity of the product has increased to a great extent.

The samples treated with air at 50 and 80% of burn-off present the reactivity profiles shown in Fig. 6. It can be observed that the A50 sample exhibits a bimodal peak with nearly the same contribution from both peaks (55% for the low temperature peak and 45% for the high temperature peak, see Table 3).

If the 50% burn-off samples are compared, it can be seen that oxidative treatment in air (A50) was more selective in the removal of the carbon material that oxidises at low temperature, as its contribution was reduced from 80% in FGA to 55% in A50. On the contrary, the treatment in CO_2 (C50) only reduces the low temperature peak contribution from 80 to 73%. Thus, the most reactive carbon form in the parent sample, FGA, is removed by air treatment to a greater extent than in CO_2. This implies that treatment with CO_2 removes both disordered and non-disordered carbon. This result can

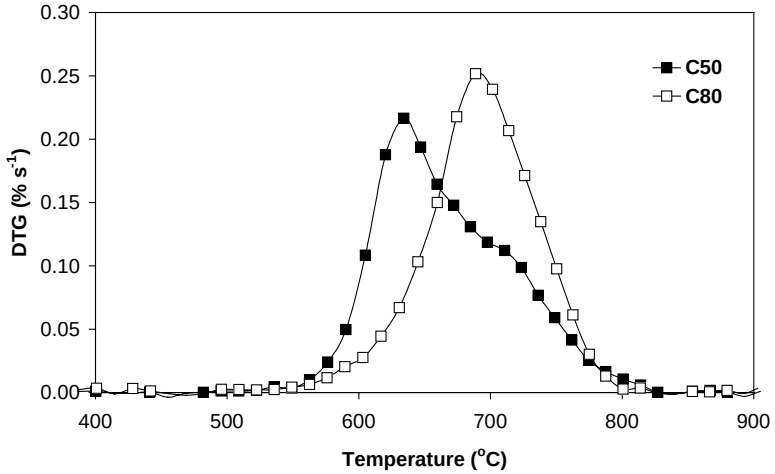

Fig. 5. DTG profiles of CO_2-treated samples.

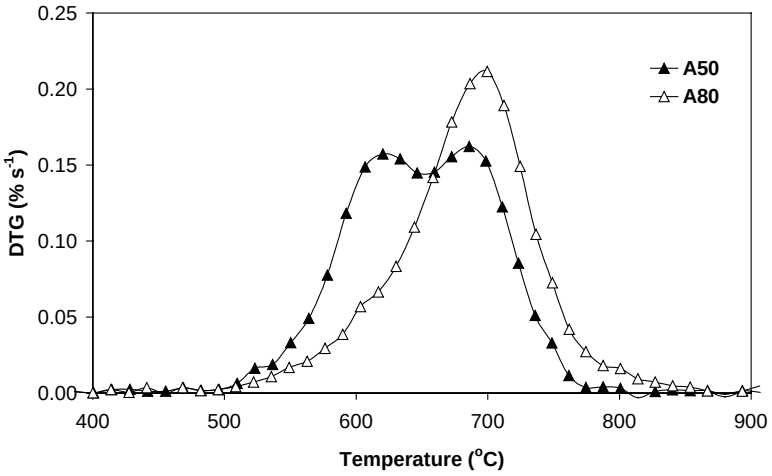

Fig. 6. DTG profiles of air-treated samples.

be explained in terms of the catalytic effect induced by the residual iron (used as catalyst for the production of the fibre) on the CO_2 gasification of the carbon constituents (both disordered and non-disordered). In the case of oxidation in air it seems that the catalytic effect of iron did not have the same influence as in the case of CO_2, either due to the deactivation of the catalyst in the stronger air oxidising atmosphere, resulting in oxidised iron species, which are poor catalysts for the gasification of carbon with oxygen and CO_2 [26], or because of deactivation through the metallic iron sintering [27]. An analysis of the X-ray diffraction patterns shown in Fig. 3 indicates that, for the samples oxidised in air, the iron is present in the form of hematite (iron oxide) while for the CO_2 oxidised samples, diffraction peaks corresponding to metallic iron were detected. This confirms the deactivation of the residual iron in the case of the air-oxidised samples.

Reaction up to 80% of burn-off seems to be more selective for the CO_2 treatment, as the profile of sample C80 in Fig. 5 shows only a very small contribution from the low-temperature peak (8%; see Table 3), while the profile of the 80% burn-off sample in air (A80) presents a contribution of 20% for the same peak. It seems that as the reaction proceeds (higher burn-off degree) uncatalysed CO_2 gasification takes on more relevance and selectively removes the most reactive carbon components of the fibres produced. This is in agreement with the results of other authors, who found that the oxidation of VGCNFs at high burn-off degrees takes place by an uncatalysed reaction mechanism [28].

One point to be considered is the possibility of the modification of the textural properties of the product with the oxidative treatments. Table 2 shows some of the textural properties of the parent and treated materials. It can be seen that neither the thermal treatment in an inert atmosphere (N600 and N900), nor the treatments in CO_2 (C50 and C80) cause any significant modification of the apparent surface area calculated according to the BET equation. Only the treatments in air seem to modify the surface area of the materials, the treated samples having about twice (A80) and three times (A50) the specific surface area of the untreated sample (FGA). This could explain why the initial mass loss, for the air treated samples, started at a lower temperature (i.e., around 500 °C; see Fig. 6) in comparison with the CO_2 treated samples (i.e., 550 °C; see Fig. 5). An analysis of the N_2 adsorption isotherms (not shown) together with the pore volume and specific surface area data (Table 2) show that treatment with air favours a general development of porosity of all sizes, while CO_2 treatment causes an increase in large pores, which provide only a small contribution to the specific surface area.

It would also be interesting to know whether the treatments cause changes in the carbon structure with respect to the original sample. The X-ray diffraction patterns of the samples are displayed in Fig. 3, and their structural data are given in Table 2. From these results it can be inferred that the graphite-like bulky structure of the treated VGCNFs remained practically unchanged, in agreement with the findings of other authors [29,30]. Also of significance is the presence of hematite (Fe_2O_3) in the samples treated with air, as well as iron in the samples treated with CO_2 and with nitrogen.

Another point to be considered is the incorporation of oxygen after the reactive treatments of the raw material. As can be seen from Table 1, all the treatments performed (i.e., in inert atmosphere, air and CO_2) produced a notable decrease in the volatile matter content of the treated product, although this does not imply a decrease in the low temperature peak. The oxygen content undergoes a slight increase while both the nitrogen and hydrogen contents decrease. These changes take place whether the treatments are performed in an oxidative atmosphere (i.e., air or CO_2) or in a nitrogen atmosphere. This suggests that the thermal effect of the treatments is more important than the actual oxidation. In other words, an increase in temperature during the treatment eliminates some of the surface groups (presumably nitrogen-containing groups), giving rise to a relatively reactive surface, which re-oxidises after

exposure to the atmosphere once the treatment is over. These changes in the surface chemistry are accompanied by a slight decrease in the pH_{PZC}, either due to the elimination of basic nitrogen-containing surface groups or to the introduction (by atmospheric re-oxidation) of new acidic oxygen-containing surface groups. In any case the *functionalisation* of the surface of the fibres due to these treatments is much less important than the changes in the relative amounts of different forms of carbon in the final product.

4. Conclusions

Temperature programmed oxidation may be a useful method for obtaining information about the homogeneity and fibre content versus amorphous carbon content of an industrial product. Under the experimental conditions established in this work the *functionalisation* of the surface of the fibres and changes in their porous texture, due to the oxidative treatments applied, are much less important than the changes produced in the relative amounts of different forms of carbon in the final product. Nevertheless treatments with air cause a higher surface area development than treatments with CO_2. Remnants of iron catalyst have a significant influence on the reactivity of the industrial product and treated samples. Thus, treatments in air give rise to Fe_2O_3, which has a small catalytic effect on the oxidation reaction. In contrast, CO_2 gasification is easily catalysed by metallic iron. At high burn-off degrees the uncatalysed CO_2 gasification selectively removes the most reactive components of the fibre. At low burn-off degrees air treatment is more selective in removing the most reactive fractions than CO_2 treatment.

Acknowledgements

The authors are grateful to Grupo Antolín Ingenería, S.A., for supporting this work.

References

[1] L. Ci, Y. Li, B. Wei, J. Liang, C. Xu, D. Wu, Carbon 38 (2000) 1933–1937.
[2] M. Endo, Y.A. Kim, T. Hayashi, K. Nishimura, T. Matusita, K. Miyashita, M.S. Dresselhaus, Carbon 39 (2001) 1287–1297.
[3] D.D.L. Chung, Carbon 39 (2001) 1119–1125.
[4] C.J. Lee, J. Park, Carbon 39 (2001) 1891–1896.
[5] R. Marangoni, P. Serp, R. Feurer, Y. Kihn, P. Kalck, C. Vahlas, Carbon 39 (2001) 443–449.
[6] L. Ci, J. Wei, B. Wei, J. Liang, C. Xu, D. Wu, Carbon 39 (2001) 329–335.
[7] M.L. Lake, Novel applications of VGCF including hydrogen storage, in: L.P. Biró, C.A. Bernardo, G.G. Tibbetts, Ph. Lambin (Eds.), Carbon Filaments and Nanotubes: Common Origins, Differing Applications? Kluwer Academic Publishers, Dordrecht, 2001, pp. 331–341.
[8] K. Arakawa, Process for preparing fine carbon fibers in a gaseous phase reaction, US Patent 4,572,813 (1986).
[9] K. Arakawa, Process for preparing fine fibers, US Patent 4,640,830 (1987).
[10] R.A. Porter, L.E. Reed, Catalytic fibrous carbon, US Patent 4,518,575 (1985).
[11] T. Morita, H. Inoue, Y. Suhara, Fine carbon fiber and method for producing the same, US Patent 2002/0058139 A1 (2002).
[12] Z. Shi, Y. Lian, F.H. Liao, X. Zhou, Z. Gu, Y. Zhang, S. Iijima, H. Li, K.T. Yue, S.L. Zhang, J. Phys. Chem. Solids 61 (2000) 1031–1036.
[13] K.L. Strong, D.P. Anderson, K. Lafdi, J.N. Kuhn, Carbon 41 (2003) 1477–1488.
[14] M.R. Smith, S.W. Hedges, R. LaCount, D. Kern, N. Shah, G.P. Huffman, B. Bockrath, Carbon 41 (2003) 1221–1230.
[15] A.C. Dillon, T. Gennett, K.M. Jones, J.L. Alleman, P.A. Parilla, M.J. Heben, Adv. Mater. 11 (1999) 1354–1358.
[16] C. Merino, G. Ruiz, P. Soto, A. Melgar, E.M. Martín, J.M. Gómez de Salazar, Influence of the carbon source on the formation of carbon nanofibres for polymer reinforcement, CD-Rom of Abstracts of the Carbon'03, Oviedo, Spain, July 2003 (ISBN 84-607-8305-7).
[17] G.G. Tibbetts, D.W. Gorkiewicz, R.L. Alig, Carbon 31 (1993) 809–814.
[18] A. Arenillas, C. Pevida, F. Rubiera, J.J. Pis, Fuel 82 (2003) 2001–2006.
[19] F. Rubiera, A. Arenillas, B. Arias, J.J. Pis, Fuel Process. Technol. 77/78 (2003) 111–117.
[20] J.B. Parra, J.C. de Sousa, R.C. Bansal, J.J. Pis, J.A. Pajares, Adsorp. Sci. Technol. 12 (1995) 51–66.
[21] L. Gurvitsch, J. Phys. Chem. Russ. 47 (1915) 805.
[22] W.H. Bragg, in: W.H. Bragg, W.L. Bragg (Eds.), X-rays and Crystal Structure, Bell and Sons, London, 1918, p. 174.
[23] P. Debye, P. Scherrer, Physik 18 (1917) 291.
[24] J.S. Noh, J.A. Schwarz, J. Colloid Interf. Sci. 130 (1989) 157–164.
[25] C.A. León y León, L.R. Radovic, in: P.A. Thrower (Ed.), Chemistry and Physics of Carbon, vol. 24, Marcel Dekker, New York, 1994, p. 213.
[26] P.L. Walker, S. Matsumoto, T. Hanzawa, T. Muira, I.M.K. Ismail, Fuel 62 (1983) 140–149.
[27] H. Ohme, T. Suzuki, Energy Fuels 10 (1996) 980–987.
[28] P. Serp, J.L. Figueiredo, Carbon 35 (1997) 675–683.
[29] M.L. Toebes, J.M.P. van Heeswijk, J.H. Bitter, A.J. van Dillen, K.P. de Jong, Carbon 42 (2003) 307–315.
[30] P. Serp, J.L. Figueiredo, P. Bertrand, J.P. Issi, Carbon 36 (1998) 1791–1799.